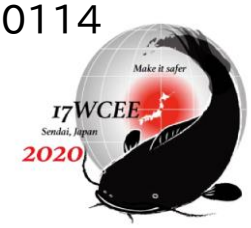

17th World Conference on Earthquake Engineering, 17WCEE
Sendai, Japan - September 13th to 18th 2020

SEISMIC BEHAVIOUR OF FULL-SIZE CONCRETE COLUMNS INTERNALLY REINFORCED WITH GLASS FRP

Z. Kharal[(1)], S.A. Sheikh[(2)]

[(1)] *Postdoctoral Fellow, Department of Civil and Mineral Engineering, University of Toronto, zahra.kharal@mail.utoronto.ca*
[(2)] *Professor, Department of Civil and Mineral Engineering, University of Toronto, sheikh@ecf.utoronto.ca*

Abstract

To address the problem of steel corrosion in reinforced concrete structures, the use of GFRP bars in full-scale columns has been investigated as an alternative to steel reinforcement for sustainable construction. As columns containing GFRP longitudinal and GFRP lateral reinforcements display softer responses with lower shear and flexural capacity compared with columns with all steel reinforcement, use of lateral GFRP reinforcement with steel longitudinal bars was investigated in an extensive research program.

The experimental program includes the design, construction and testing of full-scale concrete columns ranging up to 508 mm in diameter under constant axial load and cyclic lateral displacement excursions simulating seismic loading. A special test set-up was designed for these large columns. All the columns, discussed in this paper, were reinforced laterally with GFRP spirals and longitudinally with steel bars or GFRP bars. Variables included level of axial load, amount of confining reinforcement and spacing of transverse reinforcement. GFRP lateral reinforcement was found to provide increasing confining pressure to the large concrete core with increased deformations, even more efficiently than comparable smaller 356 mm diameter columns. Results from a select group of specimens are presented to highlight the effects of different variables and establish the feasibility of using GFRP spirals in large circular bridge columns to provide confinement.

Keywords: Column confinement; FRP; Codes; design guidelines; Seismic resistance; Ductility; Sustainable Structures

1. Introduction

Steel in conventional reinforced concrete (RC) members in bridges is prone to corrosion due to the high exposure level to relatively severe environmental conditions. Corrosion in highway bridges in North America alone causes hundreds of billions of dollar damage annually [1]. In Canada, the salt used to melt snow and ice creates conditions that accelerate the corrosion phenomenon. Bridge columns, in particular, are often found to have suffered extensive corrosion damage, sometimes even prior to half their design life.

Corrosion of lateral steel in columns causes spalling of concrete cover which results in a drop in their load-carrying capacity, ductility and energy dissipation capacity. If the corrosion damage progresses to longitudinal bars, the situation is exacerbated considerably. Columns are probably the most critical elements in bridges and the failure of even one of them in a critical location can lead to a complete bridge collapse. A large portion of this corrosion could be eliminated by utilizing various prevention techniques which will not only save billions of dollars annually in infrastructure repair but more importantly will also ensure health and safety of the public. The replacement of steel with a non-corroding material like glass fiber reinforced polymer (GFRP) bars is one feasible solution that can alleviate the problem of corrosion in columns.

During the past decade, several studies have been reported on the behaviour of GFRP bars as lateral and longitudinal reinforcement for concrete components under compression [2-4]. Based on the results of the tests, it was found that replacing longitudinal steel bars with GFRP bars, irrespective of the type of ties (steel or GFRP), reduced the capacity by about 13% [5]. Although results from the aforementioned studies provided valuable information, the small column size, limited number of variables, and the simple load pattern necessitated the need for further investigation on the performance of columns under more realistic loadings such as seismic. To this effect, an extensive experimental program was initiated at the University of Toronto in which 356 mm diameter columns confined with glass fibre reinforced polymer (GFRP) spirals were tested under simulated earthquake loading. In the first phase, nine circular columns reinforced with GFRP spirals and GFRP longitudinal bars were tested under reversed cyclic lateral load while simultaneously subjected to constant axial load [6]. While GFRP spirals were found to confine concrete better than steel spirals, the use of GFRP longitudinal bars – which had about 70% less stiffness than steel - resulted in a considerably softer column response with lower moment and shear capacities compared to steel reinforced columns. The results of phase one, prompted the need to conduct phase two, in which seven columns reinforced with conventional steel longitudinal bars and GFRP spirals with the exact same dimensions and loading configuration as the previous study were tested [7]. These hybrid columns were found to have moment capacities and ductility factors comparable to traditional steel reinforced columns. In addition, it was found that if appropriate confinement was provided, the GFRP spirals were able to provide better confinement than conventional steel spirals.

The promising results of the second phase, resulted in the third phase of the program, summarized in this paper, on larger full-scale circular columns. To provide engineers a more realistic understanding of the behavior of columns with steel longitudinal bars and GFRP spirals before being utilized in real bridges, a study on larger columns was found to be necessary. To this effect, eight columns with 508 mm diameter, reinforced with steel longitudinal bars and GFRP spirals, were used to investigate the effects of variables such as the level of axial load, amount and spacing of transverse reinforcement on full size size columns. Prior to this study, no such tests on columns this large have been reported. Several challenges were encountered and had to be dealt with during the design, construction and testing phases due to the large size of the specimens. For each column, in addition to the moment vs. curvature response and shear vs. deflection behaviour, several ductility parameters related to curvature and displacement were also used to evaluate the seismic performance of column specimens. Most importantly, performance was evaluated against the comparable smaller columns [7] with the aim of assessing whether the excellent GFRP spiral confinement behaviour found in 356 mm diameter columns will also be present in comparable full-scale columns. In this

paper, a summary of the experimental program, test set-up, selected test results and a brief discussion on the results are provided.

2. Experimental Program

2.1 Specimen details

A total of eight circular columns were constructed and tested in the Structures Laboratories at the University of Toronto. The columns were 508 mm in diameter, had a length of 1695 mm and were cast monolithically to a stub of 700 x 700 x 700 mm. The shear span to depth ratio of the columns was 4.0. The shear span was measured from the centre of the support hinge. Each column contained eight 25 mm longitudinal steel bars uniformly distributed around the column core and a GFRP spiral spanning the entire column length. The geometry of the column specimens with the reinforcement cage is shown in Fig. 1.

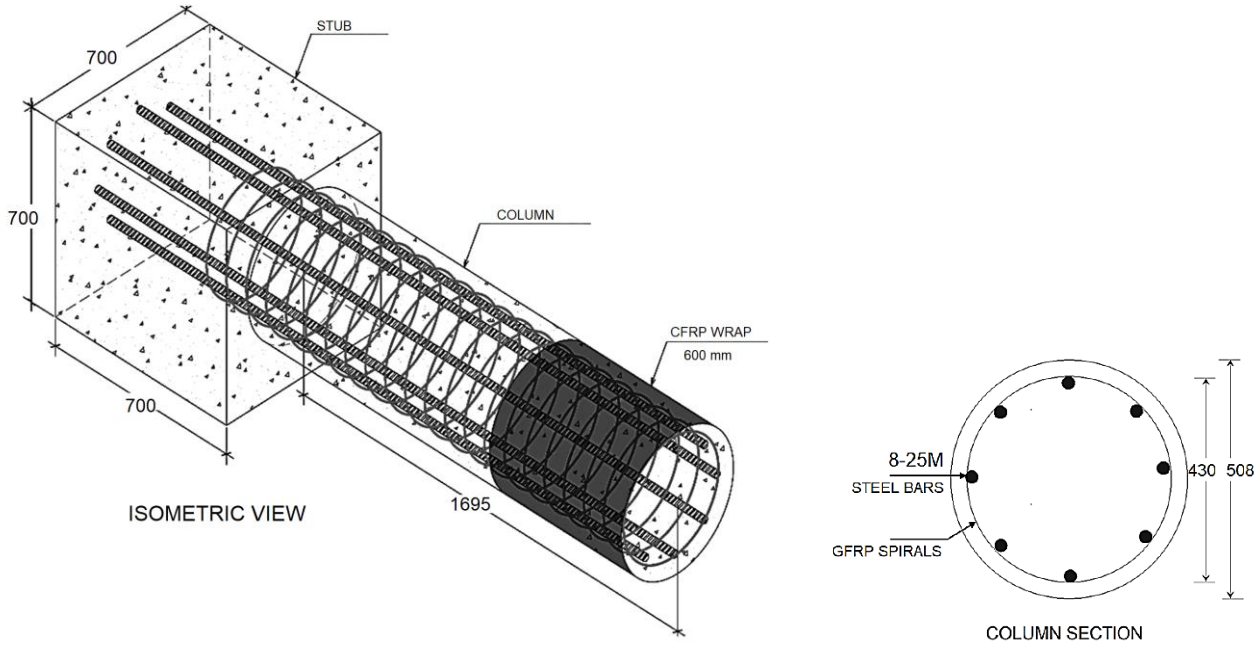

Fig. 1 – Column specimen geometry (all dimensions are in mm)

The concrete strength was specified to be 30 MPa for all specimens; at the time of column testing, the concrete strength had increased considerably to about 47 MPa. The four major variables investigated were the column diameter, size and amount of GFRP spiral, GFRP spiral spacing and level of axial load. Due to the limitation of the available space, results from only three large size columns are discussed in this paper. The details of the specimens are provided in Table 1. In addition, the details of three comparable smaller specimens [7] are also given in the table. All three smaller specimens had a diameter of 356 mm and a length of 1470 mm with the shear span to depth ratio of 5.16; the results of these specimens will be utilized later in the paper for comparison purposes. The last digit in the Specimen ID is the specimen number for easy reference.

Table 1 – Specimen Details

Study	No.	Specimen ID	Column Diameter [mm]	Compressive Concrete Strength, f_c' [MPa]	Axial Load Level, P/P_o	Spiral Diameter, Ø [mm]	Spiral Pitch, s [mm]	Lateral Reinforcement Ratio, ρ_h [%]
Current study	Ø508 mm, L = 1695 mm, Stub = 700 x 700 x 700 mm, 8-25M Longitudinal Steel Bars (2.04%)							
	2	P28-LS-12-60-2	508	47	0.28	12	60	1.65%
	3	P28-LS-12-90-3	508	47	0.28	12	90	1.10%
	7	P56-LS-12-35-7	508	47	0.56	12	35	2.83%
Tavassoli and Sheikh (2017)	Ø356 mm, L = 1470 mm, Stub = 700 x 700 x 800 mm, 6-25M Longitudinal Steel Bars (3.00%)							
	1	P55-LS-12-50-1	356	41	0.56	12	50	3.00
	5	P28-LS-12-160-5	356	41	0.28	12	160	0.94
	7	P28-LS-12-50-8	356	41	0.28	12	50	3.00

2.2 Instrumentation

Extensive instrumentation, including LVDTs and strain gauges, were used on all the specimens to gain a thorough understanding of the column behaviour. At least three GFRP spirals in each specimen were strain gauged within the potential plastic hinge region to accurately assess the effectiveness of GFRP spirals, determine the location of the highest strain zone and record the corresponding maximum strain. Additionally, four strain gauges were used on each turn of the spiral to understand the variation in confinement along the circumference of the column. A total of twenty-five LVDTs were used to record the horizontal and vertical displacements during each test and to determine strain at various locations.

2.3 Test set-up

The specimens were tested in the Column Testing Frame (CTF) in the Structures Laboratories at the University of Toronto. The original CFT used for smaller tests needed to be modified considerably in order to accommodate the larger size specimens [6, 7]. In particular, changes had to be made to the end anchor plates and the diagonal braces in the frames. Fig. 2 (a) shows the modified CTF test set-up with a fully instrumented column specimen installed. The specimens were placed in the CTF in a horizontal position and subjected to simultaneous pre-determined constant axial load and cyclic quasi-static lateral excursions simulating earthquake loading. The axial load was applied using a 10,000 kN servo controlled hydraulic jack, and an actuator with 1,000 kN (225 kip) load capacity and 200 mm displacement capacity was used to apply the lateral cyclic displacement excursions.

The axial load was maintained at the required level in the beginning of the test, following which the lateral load was applied. Lateral load was applied at the stub approximately 150 mm away from the stub-column interface, so that the most critically loaded region of the column was adjacent to the stub and subjected to combined flexure, shear, and axial forces. The lateral loading protocol followed for each test can be seen in Fig. 2 (b); where Δ_y was the theoretical displacement corresponding to the column lateral load capacity on a straight line joining the origin and the point corresponding to 65% the column capacity on the ascending part of the load-deflection curve. In the first cycle of the lateral load, a peak displacement of $0.75\Delta_y$ was applied to the specimen. This was followed by two cycles each to peak displacements of Δ_y, $2\Delta_y$, $3\Delta_y$ and so on till the applied lateral load reached 1000 kN, the capacity of the actuator in the three larger columns discussed in this paper. Once the load reached the actuator capacity, the axial load level was reduced to $0.20P_o$ in the following cycle; this load was maintained for the subsequent cycles (~ two), till the spalling of the concrete cover occurred. After the concrete cover had spalled off, axial load was increased to its original prescribed level, which was then maintained throughout the duration of the remaining test, and the lateral loading cycles

were continued to be applied till specimen failure. The specimen was considered failed when it was unable to maintain the originally applied axial load.

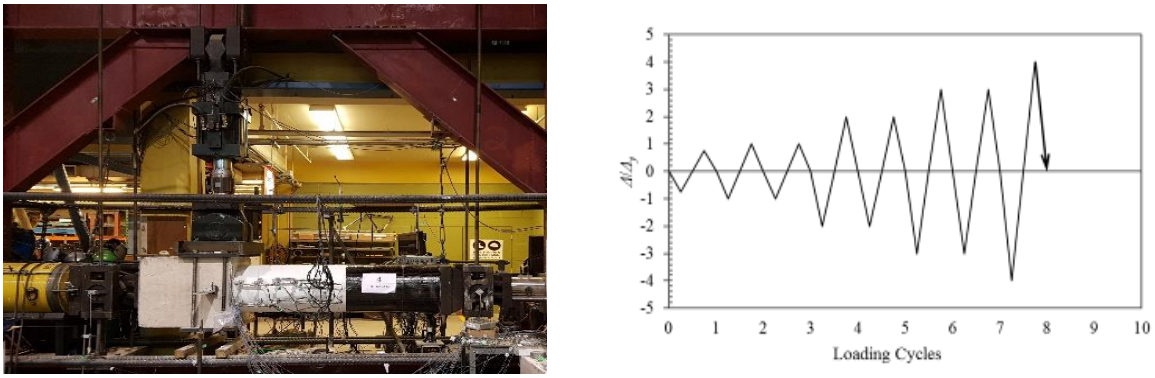

Fig. 2 – (a) CTF test set-up; and (b) Lateral loading protocol

3. Results

3.1 Observations

During the first cycle, GFRP confinement had little to no effect, and the concrete cover was visually free of any cracks. The appearance of tiny flexural cracks in the top and bottom cover at the end of the second or third cycle was the first sign of damage in all column specimens. Following this, the cover spalling initiated in the fourth cycle. Over the next several cycles, GFRP confinement became activated which continued to provide exceedingly high confining pressure until the rupture of the most stressed part of the GFRP spiral in the plastic hinge. In column specimen 3, which had a spacing of 90 mm, the specimen failed as spiral rupture occurred in conjunction with damage to the concrete core and buckling of the steel longitudinal bars. However, specimens 2 and 7, which had spacings of 60 mm and 35 mm, respectively, were able to still undergo several additional cycles after GFRP rupture. In fact, specimen 7 was able to sustain the axial load even after the rupture of the 3rd spiral turn. In comparison, similar small scaled specimens were able to sustain the axial load for a maximum of two spiral ruptures, as can be seen in Fig. 3; the ruptured spirals have been highlighted in red. Specimen group numbers are given in Table 2.

The column specimen failure details, including the most damaged region section, are given in Table 2. For the large three specimens, the spalling of the cover eventually extended to about 600-800 mm from the column–stub interface. The most damaged section was not at the column–stub interface, the section of theoretical maximum moment, but was shifted away quite a bit due to the presence of heavy confinement provided by the stub. It was observed that for large columns, the most damaged section was further from the column-stub interface in comparison to similar small columns, as shown in Table 2. In particular, for well-confined columns in Groups 1 and 3, the most damaged section for the large specimens was almost twice as far as the comparable smaller specimens.

3.2 Hysteresis response

The lateral shear versus tip deflection V–Δ and the moment versus curvature M–Φ responses at the most damaged sections were determined for all column specimens, from the beginning of the tests to the point the tests were terminated, utilizing the method and expressions used for the small-scaled specimens [7]. The resulting hysteresis responses of the three large-scale specimens are plotted in Fig. 4.

Table 2 – Failure details of columna specimens

Group	Similar	Specimen Name	Size [mm]	ρ_h [%]	Column Failure Details			Failure Mode
					Last Cycle	Most Damaged Section D_{md} [mm]	Max. Tip Displacement [mm]	
1	spacing	**P28-LS-12-60-2**	508	1.65	19	220	121	2 spirals ruptured
		P28-LS-12-50-8	356	3.00	24	110	86	1 spiral ruptured
2	reinforcement ratio	**P28-LS-12-90-3**	508	1.10	13	200	88	2 spirals ruptured
		P28-LS-12-160-6	356	0.90	12	180	57	1 spiral ruptured
3	reinforcement ratio	**P56-LS-12-35-7**	508	2.83	19	230	116	3 spirals ruptured
		P55-LS-12-50-1	356	3.00	15	140	55	2 spirals ruptured

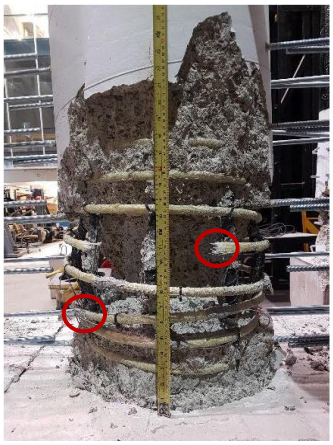

P28-LS-12-90-3: Large

P28-LS-12-160-6: Small

(a)

P56-LS-12-35-7: Large

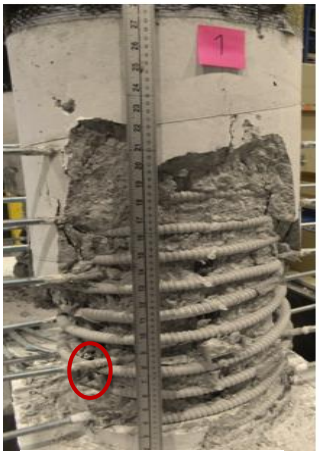

P55-LS-12-50-1: Small

(b)

Fig. 3 – Plastic hinge regions at end of testing for columns in: (a) Group 2; and (b) Group 3

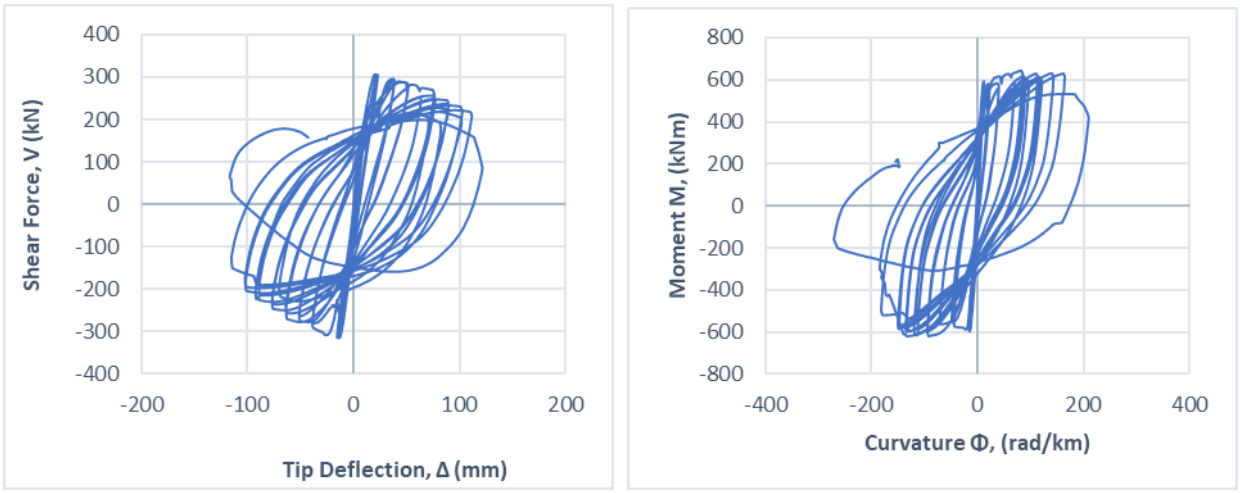

(a) Column P28-LS-12-60-2

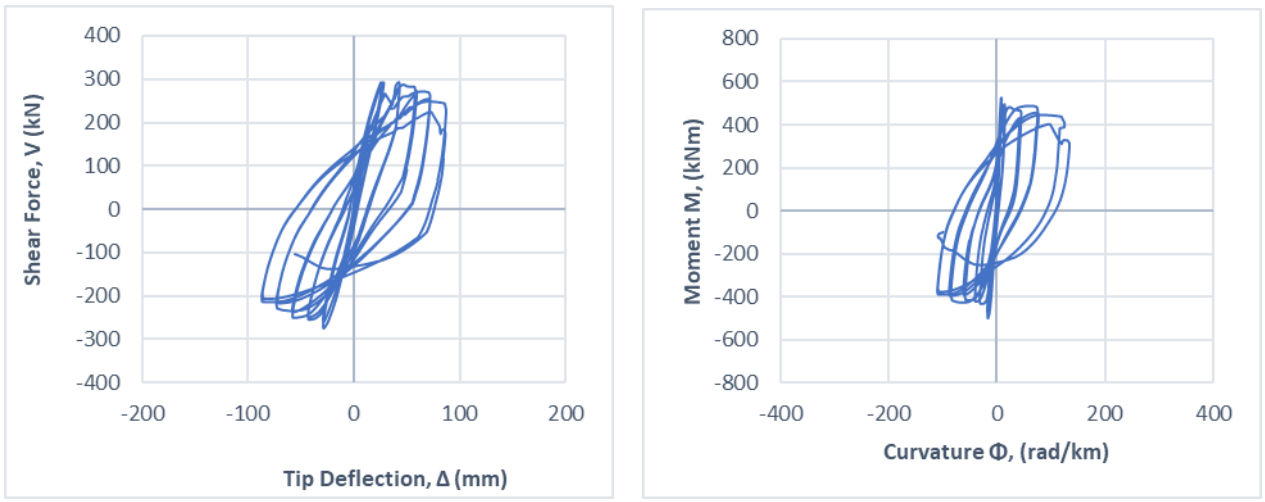

(b) Column P28-LS-12-90-3

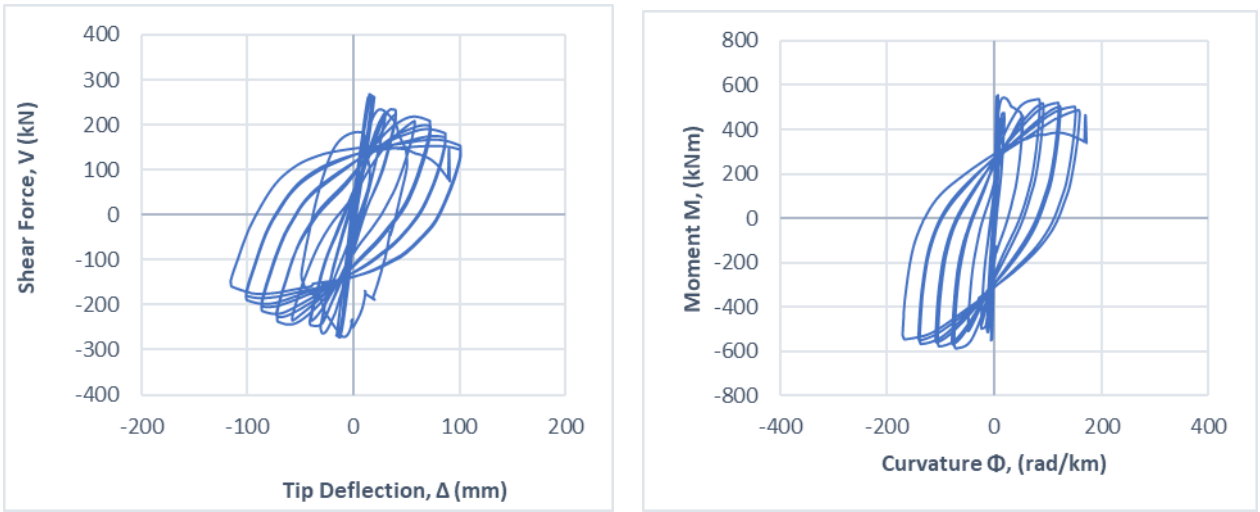

(c) Column P56-LS-12-35-7

Fig. 4 – Shear versus tip deflection V–Δ and moment versus curvature M–Φ hysteresis response

3.3 Comparison with small-scale specimens

This study was designed to ensure that several comparisons could be carried out with the smaller circular columns confined by GFRP spirals tested earlier by Tavassoli and Sheikh [7] to evaluate the validity of the GFRP spiral effectiveness in field columns. The three large and three small specimens were categorized and divided into three groups based on either a similar lateral reinforcement ratio level or spiral spacing, as shown Table 3; the specimens in Group 1 have similar spacing but different spiral ratios, the specimens in Group 2 have similar spiral ratio but different spacing and Group 3 specimens have reasonably close lateral reinforcement ratio and spacing.

3.3.1 Hystersis Response

In this section, the hysteresis response of the large column specimens is compared with that of their companion small column specimens. The maximum shear and moment capacities were found to be considerably different between the large- and small-scale specimens. To minimize the effect of the small variation in concrete strength and the difference in capacities due to column sizes, the shear was normalized with respect to the nominal shear strength values and the moment with respect to the nominal moment capacities. The nominal shear and moment capacities, V_n and M_n, have been provided in Table 3; they were determined by theoretical sectional analysis of the unconfined column sections using the actual material properties. The specimens in Group 1, with similar spacing, and Group 3, with similar lateral reinforcement ratio, have been plotted in Fig. 5.

Group 3 specimens, P56-LS-12-35-7 and P55-LS-12-50-1, have been compared in Fig. 5 (a); the latter small-scaled specimen of 356 mm was tested by Tavassoli and Sheikh [7]. Both specimens were subjected to an axial load level of about $0.56P_o$ and had similar ρ_h values, 2.83% in case of specimen 7 and 3.00% for specimen P55-LS-12-50-1. The two specimens were tested under similar test conditions. It can be seen that the large-scale specimen performed better in terms of the maximum tip deflection and the maximum curvature values attained at failure. At failure, specimen 7 underwent 19 complete cycles (tip deflection = 116 mm), and specimen P55-LS-12-50-1 underwent 15 cycles (tip deflection = 55 mm). It was noticed that the shear enhancement was a bit larger for the smaller specimen P55-LS-12-50-1 (1.19 vs 1.13), yet the deterioration in the shear strength per cycle was also larger. The observed flexural strength enhancement M/M_n decreased from 1.42 for the small column to 1.10 for the large column. It should be noted that the M–Φ hysteresis response between the small and large scaled specimens was slightly different post-spalling. After spalling, the moment of the smaller specimen increased in each subsequent cycle, with the largest moment value attained at column failure when the GFRP spiral ruptured. On the other hand, it was observed that the larger column had more or less constant moment until failure. This was due to the limited actuator capacity (1,000 kN) which caused the tests to be continued under lower axial loads until the cover was spalled off.

The V–Δ and M–ϕ curves of the two specimens in Group 1, P28-LS-12-60-2 and P28-LS-12-50-8, compared in Fig. 5 (b) show some similarity in the overall response. This is especially the case for the M–Φ plot, where both the moment enhancement and the curvature response of the large column seem very similar to those of the smaller companion column. Additionally, the two specimens had similar flexural strength enhancement values of 1.17 and 1.21 for specimens 2 and P28-LS-12-50-8, respectively. Thus, an increase in the size of columns does not seem to cause a reduction in flexural capacity if the two compared columns have the same spiral spacing. In fact, the large column was able to sustain the moment till a curvature value comparable to the smaller companion specimens. In case of the V–Δ relationship, the ratio of deterioration of the shear in each cycle seemed very similar in the two specimens. However, the smaller specimen P28-LS-12-50-8 can be seen to have a longer post-peak descending branch than the larger specimen. It should be noted that the spiral volumetric ratio was much larger in the smaller column although the spiral spacing was almost similar.

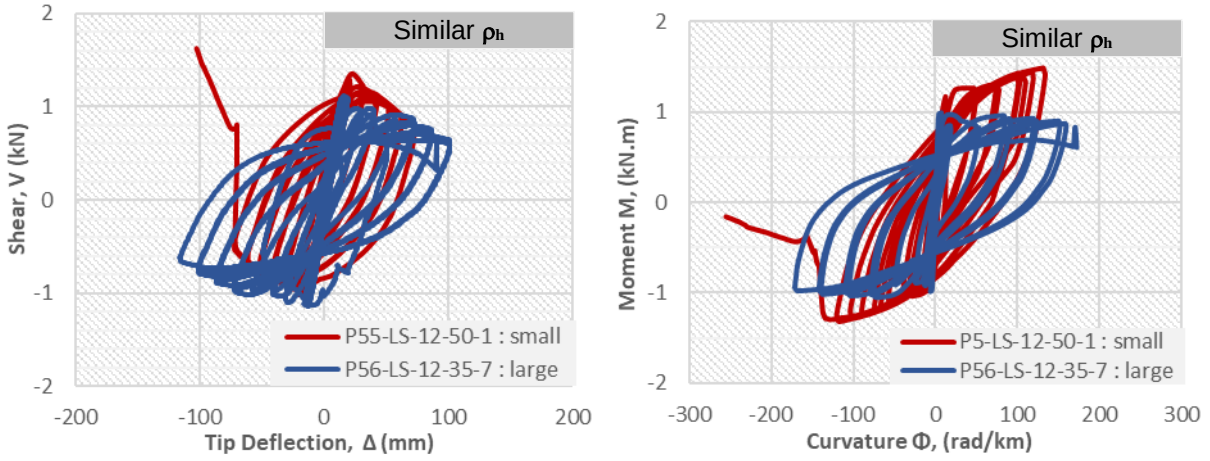

(a)

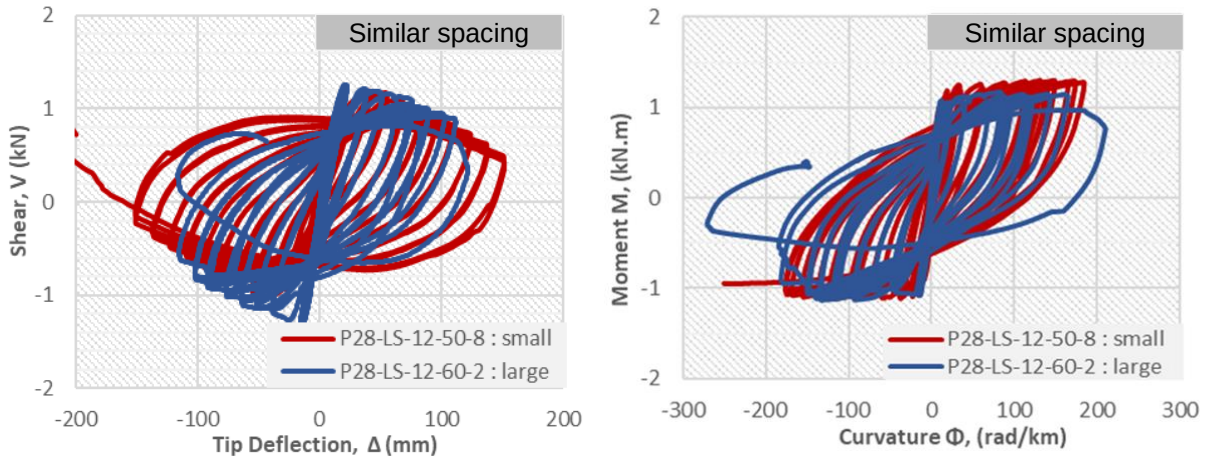

(b)

Fig. 5 – Comparison of V–Δ and M–Φ hysteresis responses of small- and large-scale specimens for (a) similar ρ_h; and (b) similar spiral spacing

3.3.2 Ductility Parameters

The ductility response of the column specimens was investigated by calculating three of the more well-known ductility parameters, displacement ductility factor μ_Δ, curvature ductility factor μ_Φ and the drift ratio δ. The μ_Δ was calculated from the V–Δ envelope curve as $\mu_\Delta=\Delta_u/\Delta_y$, where Δ_u was the ultimate displacement corresponding to the post-peak shear capacity of $0.8V_{nom}$ or the occurrence of column failure, whichever occurs first, and Δ_y is the yield displacement corresponding to V_{nom} along a straight line joining the origin and pre-peak point of $0.65V_{nom}$ on the V–Δ envelope curve. The curvature ductility factor μ_Φ was calculated in the same manner on the M–Φ envelope curve. The drift ratio was defined as Δ_u/L, where L was the total shear span of the column. The values of the three parameters have been provided in Table 3.

Table 3 – Summary of test results

Group	Specimen Name	Size [mm]	Bar@ Spacing [mm@mm]	ρ_h [%]	V_{max} [kN]	V_n [kN]	V_{max}/V_n	M_{max} [kNm]	M_n [kNm]	M_{max}/M_n	μ_Δ	μ_Φ	δ [%]
1	**P28-LS-12-60-2**	508	12@60	1.65	310	244	1.27	644	549	1.17	8.6	31.1	5.5
	P28-LS-12-50-8	356	12@50	3.00	106	96	1.10	254	210	1.21	4.7	33.8	4.7
2	**P28-LS-12-90-3**	508	12@90	1.10	283	244	1.16	524	549	0.95	5.14	16.8	4.35
	P28-LS-12-160-6	356	12@160	0.9	98	96	1.02	210	210	1.00	3.1	11.1	3.1
3	**P56-LS-12-35-7**	508	12@35	2.83	272	240	1.13	587	558	1.10	11.4	36.9	4.9
	P55-LS-12-50-1	356	12@50	3.00	95	80	1.19	266	187	1.42	4.6	26.3	3.0

For column specimens with the same amount of ρ_h and smaller spiral spacing, the test results showed that increasing the size of GFRP confined columns significantly improved the achievable section and member ductility and also increased the drift ratio that can be attained by the columns. For example, specimens' P56-LS-12-35-7 and P55-LS-12-50-1 (Group 3) were tested under similar loading conditions and were identical in almost all aspects, except that the former had a 508 mm diameter and the latter 356 mm diameter. The measured μ_Δ and μ_Φ values improved from 4.6 and 26.3, respectively, for smaller specimen to 11.4 and 36.9 for larger specimen 7. Despite an almost 147% increase in μ_Δ of specimen 7 in comparison to P55-LS-12-50-1, the corresponding improvement in μ_Φ was about 40%. Similar conclusions were reached when comparing specimens in Group 2, P28-LS-12-90-3 and Specimen 6 subjected to a lower axial load of $0.28P_o$; μ_Φ was found to increase considerably (by 51%), yet the increase in μ_Δ was even higher (by 67%). The higher ductility parameters in larger columns can be due to smaller spacing to column core diameter ratios which results in better confinement of concrete. The satisfactory μ_Φ values in all the large columns are of importance; the confinement requirements in several well-known steel design codes and guidelines, related to the demand of the seismic performance, are measured in terms of the parameter μ_Φ [8-10]. The CSA A23.3-14 Code [8] defines columns with $\mu_\Phi \geq 16$ as ductile and columns, and with $\mu_\Phi \geq 10$ as moderately ductile. While in the NZS 3101:2006 code [10], a $\mu_\Phi \geq 19$ is required to define a column as ductile and a $\mu_\Phi \geq 11$ is needed for columns to be considered to have limited ductility. Based on the aforementioned criteria, columns 2 and 7 can clearly be considered as ductile and column 3 can be categorized as either moderately ductile or ductile, based on the criteria utilized.

The drift ratio in larger columns was also higher in all the cases; the increase ranged between 17% for Group 1 to 63% in Group 3. Irrespective of the increase level, all the drift ratios were found to satisfy the criteria of the North American code requirements [8, 11]. In fact, for seismic design, a minimum drift ratio of 2.5% is required for moderately ductile columns and 4.0% for ductile columns [11, 12]. All three columns were able to attain a drift ratio that exceeded 4.0%, even the column specimen P28-LS-12-90-3, which had a spiral spacing of 90 mm and a reinforcement ratio of 1.10%. Performance of column P28-LS-12-90-3 was found to be excellent as it was under designed as per the code requirements [12]. All the values of the ductility parameters presented in Table 2 were found to be satisfactory, which shows that large scale GFRP confined columns have the ability to be very ductile and can provide confinement comparable to, if not better than, their smaller counterparts. Thus, the optimum solution with respect to column strength and stiffness, ductility and energy dissipation, and corrosion resistance, appears to be a hybrid column with steel longitudinal bars and GFRP transverse reinforcement.

4. Conclusion

This study investigates the application of corrosion resistant GFRP spirals in full-scale 508 mm diameter concrete columns under constant axial load and cyclic lateral displacement excursions simulating earthquake

forces. A summary of the results of three specimens is presented to highlight the effects of different variables on the column performance. The behaviour of these columns was studied based on the moment-curvature and shear-deflection responses and various ductility parameters in comparison with similar smaller (356 mm) column specimens.

A few of main conclusions drawn from this study have been stated below:

- The full-scale columns with GFRP spirals and steel longitudinal bars displayed stable column behavior and were able to undergo a large number of cycles and achieve high deformability levels before failure; the overall response was comparable to, if not better, than their smaller counterparts. The flexural strength and stiffness of these columns was also found to be sufficient.
- It was observed that for larger (508 mm diameter) circular columns, there was more redundancy after the rupture of the first GFRP spiral than for the comparable smaller specimens. The confinement provided to the core concrete stayed effective until the spiral ruptured at least at two locations along the column length.
- The drift capacity of all three large-scale circular columns at failure was more than 4.0%, even for columns with large spiral spacing, satisfying the requirements of the North American building codes.
- Irrespective of the column size, the optimum solution with respect to column strength and stiffness, ductility and energy dissipation, and corrosion resistance, thus, appears to be a hybrid column with steel longitudinal bars and GFRP spirals.

5. Acknowledgements

The financial support provided by the Ministry of Transportation of Ontario (MTO) and the Natural Sciences and Engineering Research Council of Canada (NSERC) is gratefully acknowledged. The authors would also like to acknowledge their gratitude and appreciation for the material support provided by Pultrall Inc, Fyfe Co. and Dufferin Concrete for this research. The experimental work was carried out in the Structures Laboratories of the University of Toronto.

6. Copyrights

7. References

[1] NACE International. (2013): Corrosion central, industries and technologies, highways and bridges. *http://www.nace.org/Corrosion-Central /Industries/Highways-and-Bridges,* Mar. 30, 2016.

[2] Tobbi, H., Farghaly, A.S., and Benmokrane, B. (2012). Concrete columns reinforced longitudinally and transversally with glass fiber-reinforced polymer bars. *ACI Struct. J*., 109(48), 551–558.

[3] Tobbi, H., Farghaly, A. S., and Benmokrane, B. (2014a). Behaviour of concentrically loaded fiber-reinforced polymer reinforced concrete columns with varying reinforcement types and ratios. ACI Struct. J., 111(33), 375–386.

[4] De Luca, A., Matta, F., and Nanni, A. (2010). Behavior of full-scale glass fiber-reinforced polymer reinforced concrete columns under axial load. *ACI Struct. J*., 107(5), 589–596.

[5] Alsayed, SH; Al-Salloum, YA; Almusallam, TH and Amjad, M A. Concrete Columns Reinforced by GFRP Rods. *Fourth International Symposium on Fiber-Reinforced Polymer Reinforcement for Reinforced Concrete Structures*, pp 188.

[6] Tavassoli, A., Liu, J. and Sheikh, S. (2015). Glass fiber-reinforced polymer-reinforced circular columns under simulated seismic loads. *ACI Struct. J*., 112(10), 103–114.

[7] Tavassoli, A., and Sheikh, S.A. (2017). Seismic Resistance of Circular Columns Reinforced with Steel and GFRP. *ASCE Journal of Composites for Construction*. Jan. 23, 2017. DOI: 10.1061/(ASCE) CC.1943-5614.0000774

[8] CSA-A23.3-14. (2014). *Design of Concrete Structures*. Canadian Standard Association (CSA), Rexdale, Ontario, Canada.

[9] Sheikh, S. A., and Khoury, S. S. (1997). A Performance-Based Approach for the Design of Confining Steel in Tied Columns. *ACI Structural Journal*, 94(4), 421-431.

[10] NZS 3101: 2006 (2017). *Concrete Structures Standard*. Standards New Zealand (NZS), Wellington, New Zealand.

[11] ACI (American Concrete Institute) (2015). *Guide for the design and construction of structural concrete reinforced with fiber-reinforced polymer (FRP) bars*. ACI 440.1R-15, Farmington Hills, MI.

[12] CSA (Canadian Standards Association). (2012). *Design and construction of building components with fibre-reinforced polymers*. CSA S806-12, Rexdale, ON, Canada, 177.

